Unexpected Sensitization Efficiency of the Near-Infrared Nd^{3+}, Er^{3+}, and Yb^{3+} Emission by Fluorescein Compared to Eosin and Erythrosin

Gerald A. Hebbink, Lennart Grave, Léon A. Woldering, David N. Reinhoudt, and Frank C. J. M. van Veggel*,†

Laboratories of Supramolecular Chemistry and Technology & MESA+ Research Institute, University of Twente, P.O. Box 217, 7500 AE Enschede, The Netherlands

Received: April 24, 2002; In Final Form: February 4, 2003

Near-infrared emissive lanthanide complexes were synthesized with covalently attached sensitizers that absorb in the visible. This functionalization was designed such that the sensitizer is in close proximity to the lanthanide ion, which is a prerequisite for efficient energy transfer from the excited sensitizer to the lanthanide ion. The sensitizers used were fluorescein, eosin, and erythrosin, which were linked via a β-alanine spacer to the polydentate chelate. The sensitizers were chosen because they absorb visible light and are structurally very similar, but the intrinsic intersystem crossing quantum yields of the sensitizers vary significantly, because of the presence of the heavy atoms (bromine in eosin and iodine in erythrosin). It was expected that an intrinsic high intersystem crossing would be beneficial in the sensitization process, because energy transfer occurs through the triplet state of sensitizers. However, because of the enhanced intersystem crossing of the sensitizers by the nearby heavy and paramagnetic lanthanide ions, these intrinsic differences were largely diminished. It was even found that fluorescein acts as a more efficient sensitizer for the NIR emission than eosin and erythrosin. The donating triplet state of fluorescein is higher in energy than that of eosin and erythrosin, resulting in less energy back transfer and therefore in a higher efficiency of sensitized emission. This and considerations of selection rules for energy transfer to the lanthanide ions made it possible to distinguish the $^4F_{9/2}$ level of Nd^{3+} as the main acceptor channel for energy transfer. In the Er^{3+} complexes, the enhancement in intersystem crossing was lower in the eosin and erythrosin complexes than in the fluorescein complex, which was concluded from the remaining complex fluorescence. Furthermore, it is tentatively concluded that additional pathways other than those allowed in Dexter energy transfer play a role in the sensitization of Er^{3+}. In the Yb^{3+} complexes, the higher efficiency of sensitization by fluorescein is due to the enhanced intersystem crossing that is larger in the fluorescein complex than in the eosin or erythrosin complex.

Introduction

Sensitized lanthanide ion emission attracts a large interest,[1] because it is an efficient way to circumvent the low absorption coefficients of these ions.[2] The main interest of this research has been focused on the visible (VIS) emission of europium and terbium,[3,4] which can be sensitized with UV absorbing sensitizers. Only in recent years has the interest shifted to the near-infrared (NIR) emissive ions, like neodymium, ytterbium, and erbium.[5−11] The use of the NIR emissive ions has a number of advantages compared to the VIS emitting ions. For instance, the emission in the NIR is ideally applicable to biology,[12] because biological tissue is relative transparent to NIR light, and to telecommunication where the ions act as active material in optical amplifiers of the NIR signals.[13] Furthermore, sensitizers that absorb in the visible region can be used here to sensitize the NIR emitting lanthanide ions.[14] This gives the advantages of cheap excitation sources such as diode lasers and the possibility to use glass instead of quartz for substrate handling in biological tests. The sensitization of these ions is still not fully understood and the search for the most efficient sensitizer−lanthanide complex combination is still ongoing.

The luminescence of the lanthanide ions originates from transitions within the partially filled 4f orbitals, which are in principle spin-forbidden.[15] Lanthanide ions with completely filled (Lu^{3+}) or unfilled (Y^{3+} and La^{3+}) 4f orbitals are not luminescent. The luminescence of the other ions ranges from the UV to the NIR. Characteristics of this luminescence are the line-like emissions, low absorption coefficients, and long intrinsic luminescent lifetimes, up to milliseconds. The energy levels of the emission are hardly effected by the environment of the ions, as the filled 5s and 5p orbitals shield the electrons in the 4f levels; in other words, the effect of the crystal field is very small.

A simplified Jablonski diagram for the sensitized emission of lanthanide ions is depicted in Figure 1. After excitation of the antenna and subsequent intersystem crossing, the energy is transferred to the lanthanide ion. In general, it is accepted that this sensitization occurs from the triplet state via a Dexter mechanism,[2] although energy transfer from the singlet state cannot be ruled out completely.[16−18] Taking the sensitization via the triplet state, the overall quantum yield of sensitized lanthanide ion emission (ϕ_{SE}) is determined by three individual steps: the intersystem crossing quantum yield (ϕ_{ISC}), the energy transfer efficiency (η_{ET}), and the lanthanide ion quantum yield (ϕ_{Ln})[19,20]

$$\phi_{SE} = \phi_{ISC}\eta_{ET}\phi_{Ln} \quad (1)$$

* To whom correspondence should be addressed. Phone: +1-250-721-7184. Fax: +1-250-472-5193. E-mail: fvv@uvic.ca.

† Current address: University of Victoria, Department of Chemistry, PO Box 3065, Victoria, BC, Canada V8W 3V6.

10.1021/jp0260090 CCC: $25.00
Published on Web 03/13/2003

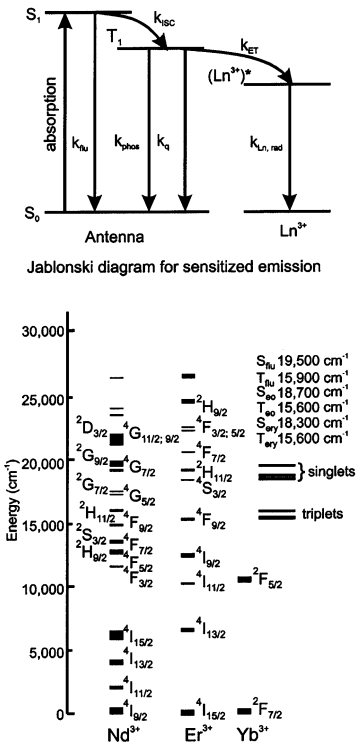

Figure 1. Top: simplified Jablonski diagram for sensitized emission; k_{flu}, rate of fluorescence; k_{ISC}, intersystem crossing rate; k_{phos}, phosphorescence rate; k_q, triplet quenching rate; k_{ET}, energy transfer rate; and $k_{Ln,rad}$, radiative decay rate. Bottom: diagram with the energy levels[25] of Yb^{3+}, Nd^{3+}, and Er^{3+} together with the singlet and triplet state energies of the three dyes (in methanol, this work[51]), "flu" stands for fluorescein, "eo" for eosin, and "ery" for erythrosin.

In the sensitization of europium, it was found that the gap between the sensitizer triplet state and the energy accepting state of Eu^{3+} has to be about 1000−2000 cm^{-1} to avoid possible energy back transfer.[21,22] This limits the sensitization to UV or violet light.[23,24] When this rule is applied to the NIR emitting lanthanide ions, it can be seen that there is in principle no limitation in the use of sensitizers that absorb in the visible. The lower limit in the triplet state energy, which will still allow for sensitized emission, will of course depend on the individual lanthanide ion (see Figure 1 for the energy levels of Yb^{3+}, Nd^{3+}, and Er^{3+}).[25] Recent work by Horrocks et al. has shown that Yb^{3+} might be excited via a photon-induced charge-transfer mechanism as an alternative pathway.[26]

A number of NIR emitting lanthanide ion complexes have been reported that have visible light absorbing antennas.[27] Some examples of these sensitizers that absorb in the visible region of the electromagnetic spectrum are fluorescein,[28,29] lissamine,[30] porphyrins,[31,32] ferrocene,[33] and ruthenium complexes.[33] However, the energy transfer pathways are still not fully understood for the sensitization of the NIR emitting lanthanide ions by these sensitizers, although it is expected that they will not differ to a large extent from those operative in the complexes with Eu^{3+} or Tb^{3+}.

For efficient lanthanide emission, complexes should have a high absorption coefficient, a high intersystem crossing quantum yield, an efficient energy transfer, and an efficient lanthanide luminescence. The absorption coefficient is not a real problem as many organic dyes and chromophores absorb strongly. Ideally, the intersystem crossing quantum yield of a sensitizer should be 100%. The intersystem crossing is enhanced by the introduction of heavy atoms such as bromine or iodine in the dye system. The energy transfer is mainly determined by the distance between sensitizer and lanthanide ion and by the normalized spectral overlap between the sensitizer and the ion (vide infra).[34]

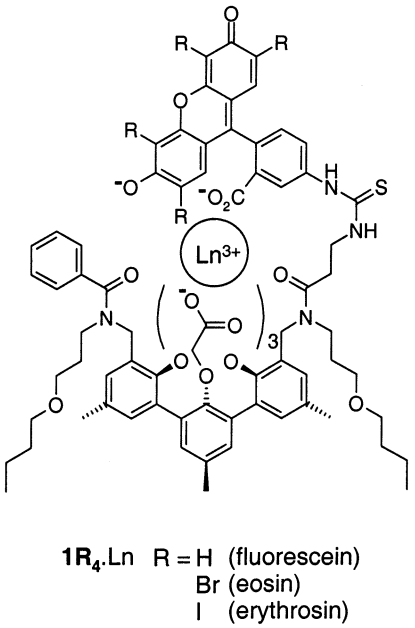

Figure 2. Terphenyl complexes functionalized with fluorescein, eosin, and erythrosin.

Here, we report the sensitization properties of NIR emitting lanthanide ions by a series of dyes based on the xanthene moiety that are structurally very similar. Complexes were made of a ligand functionalized with fluorescein, eosin, or erythrosin (Figure 2). The major difference in these dyes is the intrinsic intersystem crossing (ISC) quantum yield.[35] This difference is the result of the presence of heavy atoms in the dyes: bromine in eosin and iodine in erythrosin. This results in ISC quantum yields in water of 2% for fluorescein, 18% for eosin, and 82% for erythrosin. Furthermore, efficient energy transfer can be achieved by reducing the distance between the sensitizer and the lanthanide ion by exploiting the carboxylate group of these dyes. Because the complexes used are structurally similar, conclusions can be drawn on the effect of this inherent ISC on the sensitization properties. So far, no systematic studies have been done on the NIR emitting complexes with a series of related sensitizers. From eq 1, it would be expected that the higher the intrinsic ISC is, the better the sensitization efficiency is. However, an *external heavy atom effect* of the lanthanide ions on the intersystem crossing can be operative, thus flawing this difference.

This article is structured as follows. After the Experimental Section, the design of the complexes will be discussed with the use of molecular modeling simulations, followed by their synthesis. Then the luminescent properties in the NIR and the VIS region of these complexes will be presented. Finally, this luminescence and the energy transfer mechanism from sensitizer to ion will be discussed and conclusions will be drawn on the efficiency of sensitization of the three sensitizers.

Experimental Section

Synthesis. For a detailed description of the synthesis, see the Supporting Information to this article.

Luminescence. All measurements, except temperature-dependent measurements, were performed at room temperature or at 77 K, cooled by liquid nitrogen. The temperature-dependent measurements were performed in a temperature-controlled cell

varying between 0 and 50 °C. Absorption spectra were recorded on a HP8452A diode array spectrometer. Emission spectra in the visible and the NIR and decay traces in the visible were measured on an Edinburgh Analytical Instruments FL/FS 900 fluorimeter, equipped with a 450 W Xe lamp as steady-state excitation source and nano- and microflashlamps for time-resolved experiments. The excitation light was fed to a monochromator and focused on a square quartz cuvette (1.00×1.00 cm^2) containing the sample. The samples were prepared by dissolving the free ligand, **1R$_4$**.H_3, in methanol with subsequent addition of 1 equiv of the appropriate lanthanide ion salt (in methanol solution) and an excess of triethylamine (about 10 equiv). The emitted visible light was fed to a second monochromator and collected on a Hamamatsu R955 photomultiplier tube. Near-infrared light was fed to the same monochromator, but equipped with a 600 lines/mm grating, and was collected after optical chopping (89 Hz) by an Edinburgh Analytical Instruments liquid-nitrogen-cooled ultra-sensitive germanium detector using standard lock-in techniques. All excitation and emission spectra were corrected for the instrument spectral response. The spectral resolution was better than 1 nm for the excitation and emission spectra in the visible region. The spectral resolution of the emission spectra in the NIR was 8 nm for spectra of Yb^{3+} and Nd^{3+} and 16 nm for the spectra of Er^{3+}, and the spectral resolution on the excitation side was better than 4 nm. Lifetimes in the nanosecond regime were fitted exponentially with Edinburgh software, implemented on the instrument software, with deconvolution of the decay traces for the instrument response. This instrument response was measured on a highly scattering and nonfluorescent sample (Ludox). Lifetimes in the NIR were measured on an Edinburgh Analytical Instruments LP900 system, with a pulsed N_2 laser as the excitation source (0.5 ns pulse of a LTB MSG 400 nitrogen laser, operating at 337.1 nm at 10 Hz, pulse energy: 20 μJ). The emitted signal was collected with a North Coast liquid-nitrogen-cooled germanium detector. The decay traces were averaged by an oscilloscope (Tektronix) and fed to a computer. Fitting of the lifetimes in the microsecond region was performed with Edinburgh Analytical Instruments LP900 software, with deconvolution of the traces using the instrument response measured with IR140 (Aldrich) in methanol ($\tau < 1$ ns, much faster than the detector response, which is about 200 ns). Some typical fits are presented in the Supporting Information (i.e., a decay trace for Nd^{3+}, Er^{3+}, and Yb^{3+}). Measurements were performed on solutions with absorption below 0.3 and for quantum yield determinations absorption below 0.15. For quantum yield determinations in the visible region, $Ru(bpy)_3Cl_2$ (Aldrich) in deoxygenated water ($\phi = 0.042$) was used as a standard.[36] In the NIR, fluorexon (Molecular Probes, Leiden, The Netherlands) complexes were used (Fx.Ln, see Figure 3) as standard.[37]

Results and Discussion

Modeling. One of the advantages of this terphenyl moiety is the possibility to functionalize the building block, without altering the complexing moiety. An example of the structure of a terphenyl-based complex (Bz.Ln), without a sensitizer, is depicted in Figure 3. These complexes serve as model or reference compounds.

We have used the terphenyl moiety previously as building block for lanthanide complexes, functionalized with sensitizers.[5,30,33,38] In these reports, it was emphasized that these complexes have eight coordinating groups, leaving room for a ninth ligand on the lanthanide ion. In most cases, this place

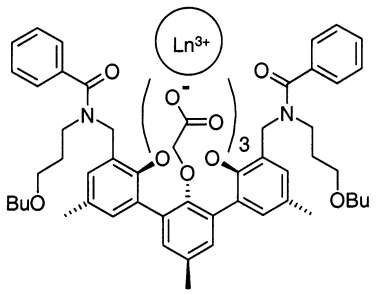

Bz.Ln

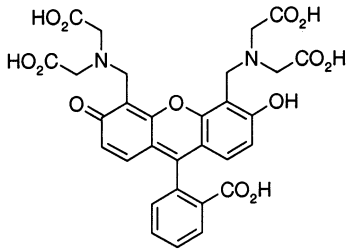

Fluorexon (Fx)

Figure 3. Molecular structures of **Bz**.Ln[46] (top) and fluorexon (Fx)[37] (bottom).

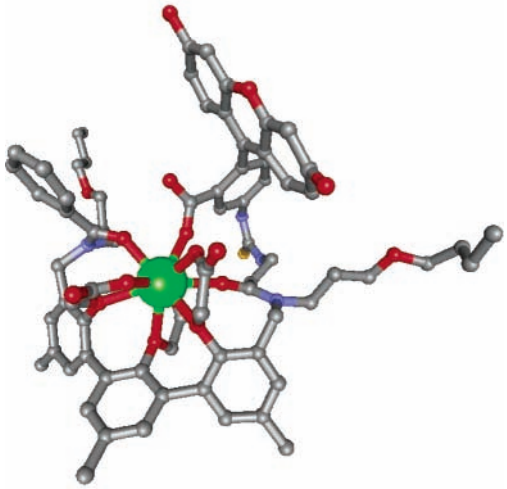

Figure 4. Snapshot of **1H$_4$**.Eu, derived from a molecular dynamics simulation in OPLS[41] methanol. Hydrogens are omitted for clarity.

was occupied by the solvent, in other cases, this place was occupied by a sensitizer, creating ternary complexes.[39] This "free" site is used here to bring the xanthene moiety of the antennas in close proximity of the lanthanide ion via coordination of its carboxylate group. A β-alanine spacer connected via an isothiocyanate moiety enables the free carboxylate of the dye to coordinate to the lanthanide ion in the ligand as was confirmed by molecular dynamics simulations for 1000 ps (see Figure 4) in OPLS methanol.[40,41] In this snapshot, the xanthene unit is at the top of the figure and the terphenyl moiety is at the bottom. The lanthanide ion is complexed by four carboxylates, two amides, and three ether oxygens leaving no room for any solvent. The average distance between the lanthanide ion and the xanthene unit[42] was determined from periodically saved sets of coordinates during the simulations. The distances found were 6.1 ± 0.2 Å for **1H$_4$**.Ln and 6.2 ± 0.1 Å for **1I$_4$**.Ln, which is much smaller than the distance of about 10 Å in similar complexes with a dye moiety attached via a rigid spacer.[43] The

SCHEME 1: i: (1) $C_2O_2Cl_2$, Room Temperature; (2) TEA, CH_2Cl_2, Room Temperature, Yield: 62%; ii: $N_2H_4.H_2O$, EtOH, Reflux, Yield: 99%; iii: TEA, CH_2Cl_2, Dye Isothiocyanate, Room Temperature, Yield: 60%; iv: TFA, Room Temperature, Yield: Quantitative

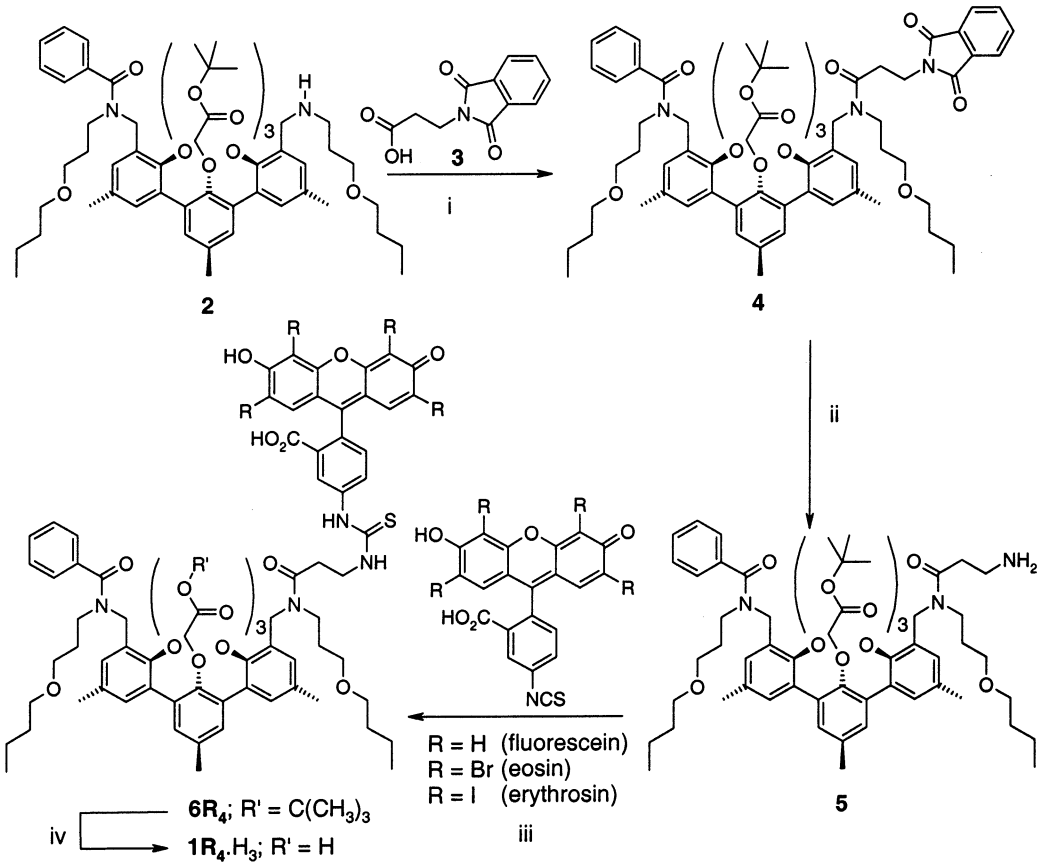

larger iodine atoms in **1I$_4$**.Ln do not influence the distance between sensitizer and ion. Furthermore, in **1I$_4$**.Ln in about half of the snapshots, a methanol was found to be in relative close proximity of the ion, 2.7 ± 0.2 Å, which is the distance between the lanthanide(III) ion and the methanol oxygen. This distance is too large for direct binding in the first coordination sphere of the lanthanide(III) ion but may act as a second sphere quencher.[44,45] The β-alanine spacer thus enables the carboxylate of the xanthene dyes to coordinate to the lanthanide ion in the complex. Doing so, the distance between sensitizer and ion is decreased and no space is left for solvents to coordinate directly to the ion.

Synthesis. The synthesis of the complexes was carried out as depicted in Scheme 1 with monoamine **2** as the starting material,[46] and a detailed description of the synthesis can be found in the Supporting Information.

β-Alanine was protected as the phthalimide **3** by heating the amino acid with phthalic anhydride, yielding **3** in almost quantitative yield. By refluxing **3** in oxalyl chloride, the acid function was converted into the acid chloride, which was subsequently reacted with monoamine **2** to yield the bisamide **4**.[46] After purification, the formation of **4** was confirmed by mass spectrometry, where a peak corresponding to **4** was found, and by the ^{1}H NMR spectrum, where no signals corresponding to protons next to an amine moiety or a carboxylic acid were found, but only signals corresponding to the amides. Furthermore, four strong peaks are found in the IR spectrum in the carbonyl region around 1700 and 1753 cm^{-1} for the esters, 1644 cm^{-1} for the amides, and 1717 cm^{-1} for the phthalimide. The deprotection of the phthalimide moiety in **4** was carried out in ethanol with hydrazine monohydrate under reflux conditions. The reaction was quantitative, and the ^{1}H NMR and IR spectra confirmed complete removal of the phthalimide. The isothiocyanate functionalized dyes were coupled to this amine **5** by stirring overnight a mixture in CH_2Cl_2 with a slight excess of dye. Purification was carried out by size separation chromatography (Sephadex), in order to remove the salts (TEA salts) and the excess of unreacted dye, and by thin-layer chromatography. Typical yields of the dye functionalized compounds **6R$_4$** (R = H, Br, or I) are in the order of 60% of the strongly colored products (absorption coefficients in the range of 77 000−84 000 L mol^{-1} cm^{-1} at the maximum between 500 and 550 nm in methanol solution). The fluorescein (**6H$_4$**) and eosin (**6Br$_4$**) compounds are highly fluorescent in solution, whereas the erythrosin compound (**6I$_4$**) exhibits much less fluorescence. The *tert*-butyl ester compounds (**6R$_4$**) were converted to the triacids **1R$_4$**.H$_3$ by mild hydrolyses in pure TFA. Complete hydrolysis was confirmed by ^{1}H NMR spectroscopy and by mass spectrometry. In the IR spectra, the resonance around 1730 cm^{-1} for the carboxylic acid is present. The purity of the compounds was checked with TLC with 15% methanol in CH_2Cl_2 as the eluent. Single spots were found with an r_F of about 0.4. The lanthanide(III) ion complexes **1R$_4$**.Ln were made in methanol by deprotonation of the ligand with 10 equiv TEA and subsequent addition of 1 equiv of lanthanide(III) nitrate salt. Complete deprotonation of the complexes, which consist of three carboxylate moieties on the terphenyl, the carboxylate on the xanthene moiety, and the phenol group on the xanthene moiety, was confirmed by UV spectroscopy, where the absorption of the dianion form of the dyes was found.[35] Complexes were made of the nitrate salts of Nd^{3+}, Yb^{3+}, and Er^{3+}, which exhibit sensitized NIR emission, and of Eu^{3+} and Gd^{3+}, which were

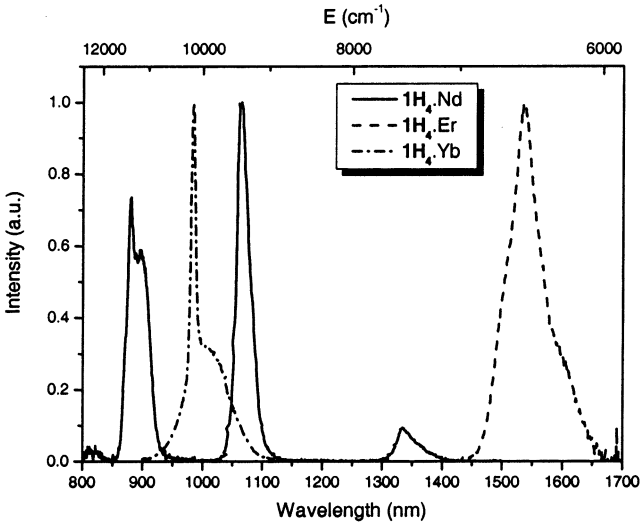

Figure 5. NIR Emission spectra of **1H$_4$**.Nd, **1H$_4$**.Yb, and **1H$_4$**.Er in CH_3OD (Nd^{3+} and Yb^{3+}) and in CD_3OD (Er^{3+}) solution.

used in addition to determine the deactivation of the singlet excited state of the dyes. The mass spectrometry characterization (ESI-TOF) data of the complexes are summarized in Table 1 of the Supporting Information. The molecular mass and the isotope pattern of the masses found correspond excellently with the calculated spectra.

Luminescence. In this section, the luminescence of the sensitizer-functionalized complexes will be described. This is done according to the simplified Jablonski diagram in Figure 1 starting with the NIR luminescence of the lanthanide ions and then the fluorescence and the phosphorescence in the visible region of the sensitizer. Finally, the energy transfer efficiency and the energy transfer rates will be discussed. The reported luminescent properties are the emission and excitation spectra, quantum yields, lifetimes, and the rates of the various transitions. The luminescence properties of Bz.Ln (Figure 3)[46] are reported in Table 2, to have a comparison. The emission in the visible region is also reported of the Gd^{3+} and Eu^{3+} complexes. These complexes (**1R$_4$**.Gd and **1R$_4$**.Eu) are a good model for the sensitizer fluorescence and phosphorescence as these ions have similar sizes as the emissive ions, and they are paramagnetic as well. However, they cannot accept energy, because the lowest excited states are too high in energy to be populated by the dyes (32 200 cm^{-1} for Gd^{3+} and 17 300 cm^{-1} for Eu^{3+}).

NIR Luminescence. *Spectra of the Nd^{3+}, Yb^{3+}, and Er^{3+} Complexes.* In the emission spectra (Figure 5), the typical emission lines for Nd^{3+} at 890 ($^4F_{3/2} \rightarrow {}^4I_{9/2}$), 1064 ($^4F_{3/2} \rightarrow {}^4I_{11/2}$), and 1330 nm ($^4F_{3/2} \rightarrow {}^4I_{13/2}$),[47] for Er^{3+} at 1536 nm ($^4I_{13/2} \rightarrow {}^4I_{15/2}$), and for Yb^{3+} at 980 nm ($^2F_{5/2} \rightarrow {}^2I_{7/2}$) are present. The emission of the **1H$_4$**.Ln complexes is shown here as representative for the emission of the other complexes (**1Br$_4$**.Ln and **1I$_4$**.Ln). The absorption and excitation spectra of the Nd^{3+} complexes are shown in Figure 6 as representative for all absorption and excitation spectra. The absorption maxima of these dyes are 505 nm for fluorescein, 535 nm for eosin, and 545 nm for erythrosin (measured in methanol solution), which are red shifted by about 5−10 nm compared to the absorption maxima of these dyes in water.[29] The resemblance of the excitation spectra to the absorption spectra proofs the sensitized emission by the dyes.

Overall Quantum Yield (ϕ_{SE}). Quantum yields of sensitized emission in deuterated methanol (ϕ_{SE}) were determined by using Fx.Nd and Fx.Yb (Figure 3)[37] as a standard for the Nd^{3+} and Yb^{3+} emission, respectively, and they are tabulated in Table 1.

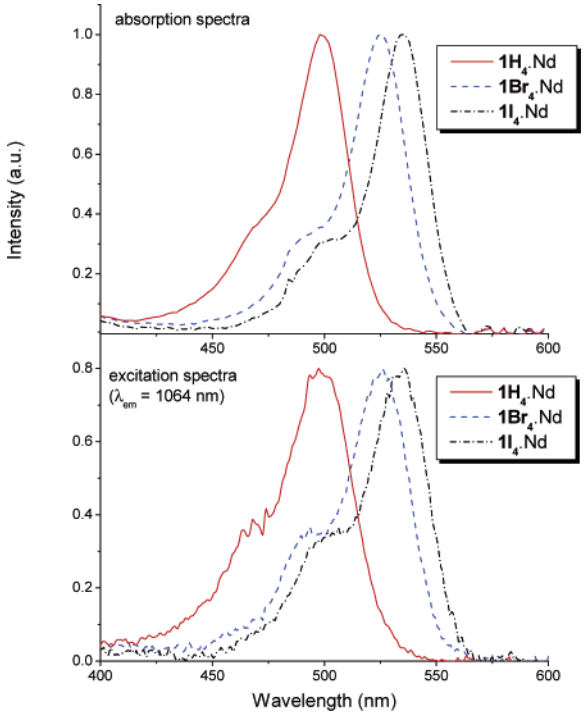

Figure 6. (Normalized) absorption (top) and excitation spectra (bottom) of **1H$_4$**.Nd, **1Br$_4$**.Nd, and **1I$_4$**.Nd in CD_3OD solution. The excitation spectra were collected by measuring the emission at 1064 nm.

TABLE 1: NIR Emission Sensitization Properties 1R$_4$.Ln (with R = H, Br, and I and Ln^{3+} = Yb^{3+}, Nd^{3+}, and Er^{3+})[a]

complex	$\phi_{SE,rel}$[b]	ϕ_{SE}[c]	τ (μs)[d]	τ (μs)[e]	ϕ_{Ln}[f]	$\phi_{ISC}\eta_{ET}$[g]
1H$_4$.Yb	0.52	2.3×10^{-3}	11.1	9.8	5.5×10^{-3}	0.42
1Br$_4$.Yb	0.32	1.4×10^{-3}	11.2	11.6	5.6×10^{-3}	0.25
1I$_4$.Yb	0.37	1.7×10^{-3}	11.5	10.2	5.8×10^{-3}	0.29
1H$_4$.Nd	0.78	3.0×10^{-4}	0.41	0.24	1.6×10^{-3}	0.19
1Br$_4$.Nd	0.37	1.4×10^{-4}	0.41	0.36	1.6×10^{-3}	0.09
1I$_4$.Nd	0.31	1.2×10^{-4}	0.37	0.25	1.5×10^{-3}	0.08
1H$_4$.Er	1.00[h]		0.91	nd	6.5×10^{-5}	
1Br$_4$.Er	0.51[h]		nd[i]	nd		
1I$_4$.Er	0.43[h]		nd[i]	nd		

[a] Properties determined in deuterated methanol, unless stated otherwise. [b] Relative quantum yield, with $\phi_{Fx.Ln}$ =1.0; error (from triplos), ±5%. [c] Absolute quantum yield, calculated from absolute quantum yield of fx.Ln: $\phi_{SE} = \phi_{SE,rel}\phi_{fx.Ln}$, $\phi_{fx.Yb} = 4.5 \times 10^{-3}$; $\phi_{Fx.Nd} = 3.8 \times 10^{-4}$; estimated error, ±5%.[37] [d] Luminescent lifetime of the lanthanide(III) ions in methanol-d_1; error, ±5%. [e] Luminescent lifetime of the lanthanide(III) ions in methanol; error, ±5%. [f] Calculated from $\phi_{Ln} = \tau/\tau_{rad}$, where τ_{rad} is the pure radiative lifetime of Ln ($\tau_{rad,Nd}$ = 0.25 ms, $\tau_{rad,Yb}$ = 2.0 ms, $\tau_{rad,Er}$ = 14 ms).[6,13,49] [g] Efficiency of the sensitization process: ($\phi_{ISC}\eta_{ET}$) = ϕ_{SE}/ϕ_{Ln}; error, ±10%. [h] Relative quantum yield, ϕ_{rel}(**1H$_4$**.Er), is set to 1, no accurate standard available. [i] nd: not determined. No accurate decay trace could be obtained.

The luminescence **1R$_4$**.Er was only measured relative to **1H$_4$**.Er because no comparison with Fx.Er standard was available. The relative quantum yields ($\phi_{SE,rel}$) show that for all three lanthanide ions the quantum yields are somewhat lower than that for Fx.Ln. A striking observation is that the complexes with fluorescein as the sensitizer have the highest quantum yields. At first glance this is in contrast with the fact that fluorescein has the lowest intrinsic intersystem crossing quantum yield, and the reason for this is presented in the discussion section. Despite the deuterated solvent, the ϕ_{SE}'s are rather low, which is mainly caused by vibrational modes within the complex itself. These quench the excited state of the lanthanide(III) ions, and this is commonly observed in organic complexes of these NIR emitting ions. In

TABLE 2: Lanthanide Luminescent Lifetimes of Bz.Ln (Figure 3),[46] in μs; Error, ±5 %

Ln^{3+}	CH_3OH	CD_3OD	$k_{q,solv}$[a]
Yb^{3+}	2.47	10.9	3.1×10^5 s^{-1}
Nd^{3+}	0.27	0.73	2.3×10^6 s^{-1}
Er^{3+}	nd	1.53	-

[a] Determined according to $k_{q,\ solv} = 1/\tau_{CD3OD} - 1/\tau_{CH3OH}$.

fact, the highest quantum yield reported for Nd^{3+} in organic solution is only 0.03, measured in a completely fluorinated ligand and in a perdeuterated solvent.[7]

Quantum Yield of NIR Lanthanide(III) Emission (ϕ_{Ln}). The quantum yields of lanthanide emission were calculated from the ratio of the measured lifetimes and the radiative lifetimes of the ions. Luminescent lifetimes of the lanthanide(III) ion complexes in the NIR were determined in normal and deuterated methanol and these are also reported in Table 1. For comparison, the luminescent lifetimes of Bz.Ln (Ln^{3+} = Yb^{3+}, Nd^{3+}, and Er^{3+}, Figure 3) are reported in Table 2.[46] The lifetimes of the ytterbium complexes **1H$_4$**.Yb, **1Br$_4$**.Yb, and **1I$_4$**.Yb are about 11 μs in both deuterated methanol and normal methanol. A rate constant of quenching by the solvent of these complexes ($k_{q,\ solv} = 1/\tau_{CH3OH} - 1/\tau_{CD3OD}$) is $\leq 3 \times 10^4$ s^{-1}, whereas the quenching by the solvent in Bz.Yb is in the order of 3×10^5 s^{-1}. This means that the ligand and coordinating sensitizer shield the ion very well from the solvent, which is in agreement with the molecular modeling studies performed on these complexes. The lifetimes of **1R$_4$**.Nd are comparable to each other, about 0.4 μs in deuterated methanol and about 0.3 μs in methanol. From this weak solvent effect, it is concluded that no solvent is coordinating to the ion. The quenching rate by the solvent for **1R$_4$**.Nd is $\leq 1 \times 10^6$ s^{-1}, caused by the quenching of solvent vibrations in the second coordination sphere. In comparison, the quenching of Bz.Nd, with first sphere solvent molecules, is about 2.3×10^6 s^{-1}. The gap between the lowest excited state and the highest ground state of Yb^{3+} (~10 200 cm^{-1}) is much larger than the gap in Nd^{3+} (~5000 cm^{-1}), which makes Yb^{3+} less sensitive to high energy vibrations of the organic environment than Nd^{3+}.[8,48] Furthermore, second-sphere coordination solvents can be more important in the Nd^{3+} complexes, because Nd^{3+} is a larger ion than Yb^{3+} allowing more space for second sphere quenchers. The lifetime of **1H$_4$**.Er in deuterated methanol is about 0.9 μs, which is comparable with the Er^{3+} lifetimes in other reports.[8,29,46,38] The lifetimes of the other complexes could not be determined, because of the low intensity of the collected traces. From these measured lifetimes and the radiative lifetimes of the ions, the quantum yields of lanthanide emission were determined. The radiative lifetimes were taken from the literature,[6,13] where they were calculated to be 2000 μs for Yb^{3+} and 14 000 μs for Er^{3+}. The radiative lifetime for Nd^{3+} was estimated to be 250 μs.[49] From this, it follows that Yb^{3+} has the largest intrinsic quantum yield (5.5×10^{-3}), then Nd^{3+} (1.6×10^{-3}), and Er^{3+} the lowest (6.5×10^{-5}). This significantly lower quantum yield of Er^{3+} was observed previously in organic complexes and is caused by the efficient quenching by C−H vibrations of the long-lived excited state of erbium[50] and probably also by inefficient sensitization (vide infra).

The efficiency of sensitization (as the product of intersystem crossing and energy transfer) is calculated from ϕ_{SE}/ϕ_{Ln} (Table 1). The efficiency of Yb^{3+} sensitization is higher than the efficiency of Nd^{3+} sensitization. Furthermore, fluorescein is a more efficient sensitizer for Nd^{3+} and for Yb^{3+} luminescence than eosin and erythrosin, despite the lower intrinsic intersystem crossing quantum yield of fluorescein. Although the efficiencies for energy transfer could not be calculated for the Er^{3+} complexes, it is clear from the relative quantum yields ($\phi_{SE,rel}$) that also here fluorescein is a better sensitizer for erbium luminescence than the other two sensitizers. However, the effect of the more efficient sensitization by fluorescein is the strongest in the case of the neodymium acceptor.

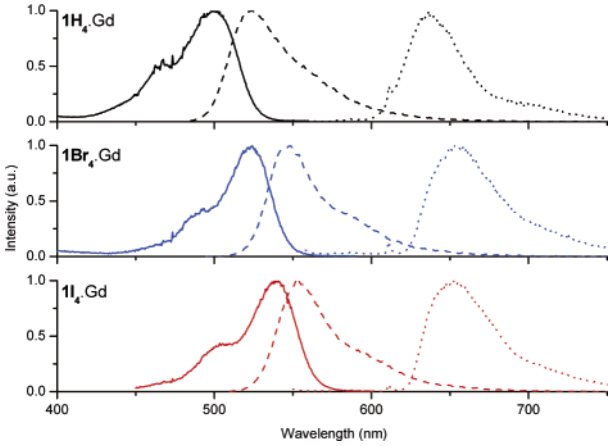

Figure 7. Excitation, fluorescence (in CH_3OH), and phosphorescence spectra of **1R$_4$**.Gd. The phosphorescence was measured at 77 K in MeOH/EtOH (1:4) glass with a delay between excitation and emission to distinguish from fluorescence.

VIS Luminescence. *Fluorescence and Phosphorescence Spectra.* The excitation, fluorescence, and phosphorescence spectra of **1H$_4$**.Gd, **1Br$_4$**.Gd, and **1I$_4$**.Gd are depicted in Figure 7. The excitation spectra of the three dyes are similar to the absorption spectra (shown in Figure 6). The maxima of the fluorescence are around 510 nm (**1H$_4$**.Gd), 540 nm (**1Br$_4$**.Gd), and 550 nm (**1Br$_4$**.Gd), red shifted by about 10−15 nm (200−400 cm^{-1}) compared to the spectra in water.[29,51] The fluorescence spectra of all of the other complexes **1R$_4$**.Ln and of **6R$_4$** have the same shape as the **1R$_4$**.Gd^{3+} spectra, but they vary in intensities. This shows that the ions do not effect the transitions energetically. Fluorescence lifetimes were determined and are 4.3 ns for **6H$_4$**, 2.5 ns for **6Br$_4$**, and 0.4 ns for **6I$_4$**. The fluorescent lifetimes of the complexes **1R$_4$**.Ln were all shorter than the detector response: shorter than about 0.3 ns. Applying the approximation that this is completely due to the enhancement of the intersystem crossing, it follows that $k_{ISC} \approx 1/\tau_{flu,complex} - 1/\tau_{flu,freedye}$, thus $k_{ISC} \geq 3 \times 10^9$ s^{-1}. The phosphorescence of **1R$_4$**.Gd^{3+} was detected at 77 K in an ethanol−methanol glass, with a delay between excitation and emission.[52] The peak of the phosphorescence is located at 640 nm for **1H$_4$**.Gd and at 660 for **1Br$_4$**.Gd and **1I$_4$**.Gd, which is also red shifted by about 10−15 nm compared to the phosphorescence of the dyes in water. The lifetimes of the phosphorescence of the **1R$_4$**.Gd complexes at 77 K were determined to be 1.6 ms for **1H$_4$**.Gd, 2.0 ms for **1Br$_4$**.Gd, and 1.5 ms for **1I$_4$**.Gd. Of all the other complexes, phosphorescence was only observed for **1R$_4$**.Eu^{3+}. The Gd^{3+} and the Eu^{3+} complexes exhibit phosphorescence, because there are no energy levels of these ions that can accept energy from the triplet states of the dyes. The absence of phosphorescence in the other complexes is due to energy transfer from the triplet states to the Nd^{3+}, Yb^{3+}, and Er^{3+} ions. At room temperature, no phosphorescence of any complex could be detected. The decrease in **1R$_4$**.Gd fluorescence is accompanied by an increase in **1R$_4$**.Gd phosphorescence, i.e., because of an external heavy atom effect. To get an estimate of the triplet state depopulation rate ferrocene, a triplet quencher was added to the solutions. Upon addition of ferrocene the NIR luminescence was quenched indeed, and a Stern−Volmer plot (data

TABLE 3: Fluorescence Quantum Yields of the Lanthanide Complexes (in %); Error, ±5 %[a]

R	$6R_4$	**1R₄**.Gd	**1R₄**.Yb	**1R₄**.Nd	**1R₄**.Er	**1R₄**.Eu
H	83	8.8	6.8	0.3	2.6	1.4
Br	76	33	30	2.6	20	23
I	8.4	6.3	7.4	1.2	5.6	4.3

[a] The fluorescence quantum yields were determined in methanol with $Ru(bpy)_3$ in deoxygenated water as a standard.

not shown) revealed a lower estimate of the energy transfer rate of about 10^8 s^{-1}.

Quantum Yield of Dye Fluorescence. Fluorescence quantum yields of the sensitizers were determined for the NIR emitting lanthanide complexes and **6R₄**, and they are presented in Table 3. These *tert*-butyl protected compounds were used as representative of the inherent dye fluorescence. The fluorescence of fluorescein is reduced from about 85% in **6H₄** to 1−5% in the complexes. The same behavior is found for the eosin (**6Br₄**) and erythrosin (**6I₄**) compounds, albeit to a smaller extent. The decreases in fluorescence upon complexation are from 76% in **6Br₄** to 2.6% in **1Br₄**.Nd, 30% in **1Br₄**.Yb, and 20% in **1Br₄**.Er and from 8.4% in **6I₄** to 7.4% in **1I₄**.Yb, 1.2% in **1I₄**.Nd, and 5.6% in **1I₄**.Er. The decrease in the fluorescence of the dyes is due to the enhancement in intersystem crossing, caused by the nearby paramagnetic lanthanide ions.[5,30,53] This conclusion is further corroborated by the fact that the dye fluorescence is reduced to the same extent in the Gd^{3+} and the Eu^{3+} complex and because of the presence of phosphorescence in these complexes. The Gd^{3+} and Eu^{3+} ions cannot accept energy from both the singlet and triplet excited states of the dyes, because the lowest excited states of the lanthanide ions are too high in energy. The small differences in the fluorescence quantum yields with varying lanthanide ion can be explained by variation in atomic weight and magnetic moment of the ions.[53,54] Although the fluorescence in the **1R₄**.Nd complexes is quenched almost completely, the **1H₄**.Yb and **1H₄**.Er complexes are quenched stronger than **1Br₄**.Yb, **1Br₄**.Er, **1I₄**.Yb, and **1I₄**.Er. This difference is of importance in the sensitization efficiency as discussed below.

Energy Transfer. The acceptor levels of the lanthanide ions are important in determining the energy transfer mechanisms from dye to lanthanide ion. A choice of potential accepting levels can be made based on the energy difference between donor (sensitizer) and acceptor level (Ln^{3+}), which should not be too large for sufficient spectral overlap,[22] and on the selection rules for energy transfer. Malta et al. performed theoretical analysis of Eu^{3+} and Sm^{3+} luminescence.[2,55] The selection rules for energy transfer from sensitizer to the Ln^{3+} $^{(2S+1)}\Gamma_J$ 4f levels are $|\Delta J| = 2, 4, 6$ for the dipolar and multipolar energy transfer (Förster type) and $|\Delta J| = 0, 1$ (but forbidden for $J = J' = 0$) for the electron exchange mechanism (Dexter type). It should be noted that these rules are (somewhat) relaxed by mixing or "stealing" from allowed transitions (e.g., 4f−5d transitions).[56] In this work, energy transfer takes place from the triplet excited state, because the singlet state of the dyes are depopulated very fast to the triplet state and the Dexter type of transfer is in general the dominant mechanism.[2,55]

Energy Transfer to Nd^{3+}. Applying these considerations to fluorescein, eosin, and erythrosin and Nd^{3+}, the levels that are expected to accept energy are the $^4F_{7/2}$ (at 13 400 cm^{-1}) and $^4F_{9/2}$ (at 15 000 cm^{-1}) levels for all three dyes (Figure 1).[57] The unlikeness of the $^4F_{7/2}$ level as acceptor level can be illustrated with a calculation of the spectral overlap of the Nd^{3+} absorption and the sensitizers phosphorescence spectra. The spectral overlap

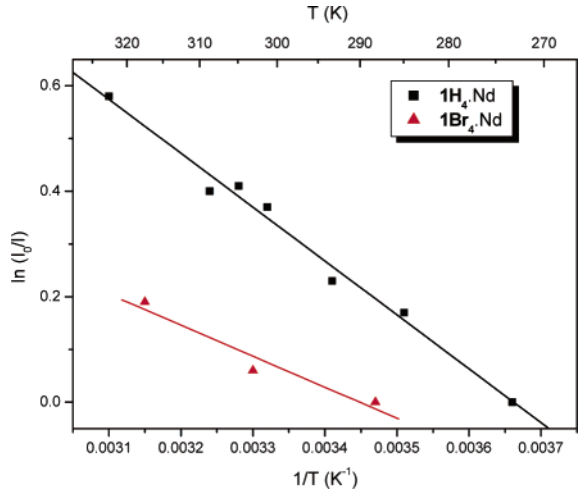

Figure 8. Plot of $\ln(I_0/I)$ versus $(1/T)$ of the NIR luminescence of **1H₄**.Nd and **1Br₄**.Nd, where I is the integrated emission intensity of the $^4F_{3/2} \rightarrow {}^4I_{11/2}$ transition around 1066 nm and excitation at 505 nm (**1H₄**.Nd) or 530 nm (**1Br₄**.Nd) in CD_3OD.

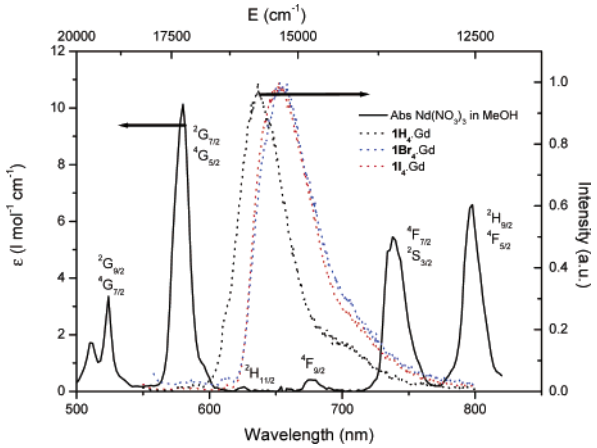

Figure 9. Phosphorescence spectra of **1R₄**.Gd at 77 K in a MeOH/EtOH (1:4) glass and part of the absorption spectrum of a 0.2 M $Nd(NO_3)_3$ solution in MeOH.

TABLE 4: Spectral Overlap Integral J of Fluorescein, Eosin, and Erythrosin Phosphorescence with the $^4F_{9/2}$ and $^4F_{7/2}$ Nd^{3+} Absorptions

	$^4F_{9/2}$	$^4F_{7/2}$	$^4F_{9/2}/F_{7/2}$
fluorescein	0.47×10^{-2}	0.08×10^{-2}	5.9
eosin	0.97×10^{-2}	0.17×10^{-2}	5.7
erythrosin	1.0×10^{-2}	0.15×10^{-2}	6.7

(J) of the dye phosphorescence and the absorption of Nd^{3+} (see Figure 9) of the $^4F_{7/2}$ and the $^4F_{9/2}$ levels is calculated according to $J = \int \epsilon(\lambda)\, F(\lambda)\, d\lambda$,[34] with the absorption of each accepting transition ($\int \epsilon(\lambda)\, d\lambda$) and the phosphorescence ($\int F(\lambda)\, d\lambda$) normalized to 1. The results of these calculations are summarized in Table 4. These calculations show that the spectral overlap of the dyes is about six times higher with the $^4F_{9/2}$ absorption than the spectral overlap with the $^4F_{7/2}$ absorption. From this, it is concluded that the $^4F_{9/2}$-energy level of Nd^{3+} is the main channel for energy transfer from these three dyes.[58] It should be noted that for both transitions ($^4F_{9/2}$ and $^4F_{7/2}$) the spectral overlap with fluorescein is a factor 2 smaller than with eosin and erythrosin. An increase of the temperature of the solutions gave a substantial decrease in the luminescence intensities of Nd^{3+}. The reason for this could be an energy-back transfer mechanism, which is supported by the fact of the relative small energy-gaps between the triplet states and the

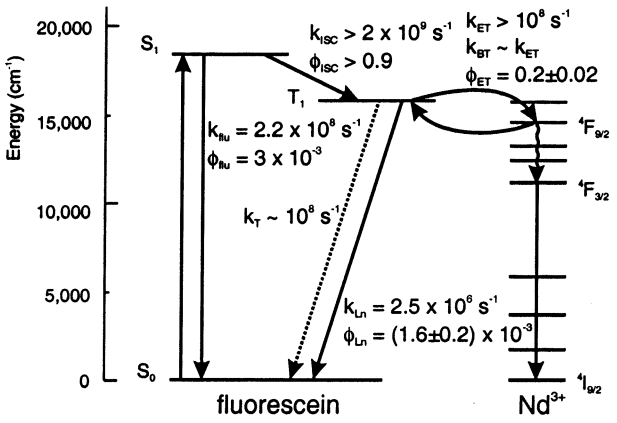

Figure 10. Jablonski diagram of the sensitization of Nd^{3+} by fluorescein (**1H$_4$**.Nd), with the rate constants and efficiencies of the various transitions.

accepting level of Nd^{3+} (700 cm^{-1} for fluorescein and 400 cm^{-1} for eosin and erythrosin). The results of variations in the temperature on the luminescence intensities are plotted in Figure 8 for **1H$_4$**.Nd and **1Br$_4$**.Nd. The luminescence of the **1H$_4$**.Nd complex *decreased* about 40% going from 0 to 50° C. The **1Br$_4$**.Nd also showed a *decrease* in intensity as well, about 20% going from 15 to 45° C. The slope in a plot of $\ln(I_0/I)$ versus $1/T$ is the energy gap ($\Delta E/k$) between the donor state (from Nd^{3+}) and the acceptor state (the triplet state of the dyes) because $I_0/I \sim k_{BT} = Ae^{(-\Delta E/kT)}$ where I_0/I is the reciprocal of the normalized luminescence intensity, k_{BT} is the back transfer rate, A is a constant, ΔE is the energy gap (in J), k is the Bolzmann constant, and T is the absolute temperature.[59] The slopes (Figure 8) correspond to an energy gap of 700 cm^{-1} in the **1H$_4$**.Nd complex and 400 cm^{-1} in the **1Br$_4$**.Nd complex. This difference between the two complexes (i.e., 300 cm^{-1}) is about the same as the difference in the position of the phosphorescence maxima, which shows that the main accepting level of Nd^{3+} is the same for both complexes.[60] This is corroborated by the calculation of the spectral overlap.

All rate constants and efficiencies of the sensitization of Nd^{3+} by fluorescein (in the **1H$_4$**.Nd complex) are summarized in the Jablonski diagram in Figure 10. After excitation, the singlet level is depopulated very fast to the triplet state. From this triplet state, the energy is transferred to the $^4F_{9/2}$ level of Nd^{3+}. This level deactivates nonradiative to the emissive $^4F_{3/2}$ level (internal conversion) or by energy-back transfer to the fluorescein triplet state. From the $^4F_{3/2}$ level, the neodymium luminescence is observed at 890, 1066, and 1330 nm.

Er^{3+} and Yb^{3+} Sensitization. Applying the same selection rules to the sensitization of Er^{3+}, only one level can be assigned that allows for excitation via an exchange mechanism, i.e., the $^4I_{13/2}$ at 6500 cm^{-1}. This implies that the energy gap between the triplets of the sensitizers and the accepting level is very large, which would result in a very small k_{ET}. Additional pathways, because of relaxation of the selection rules, may be the reason for sensitization of this ion. An additional pathway in the case of fluorescein sensitization may be one of the reasons of the more efficient sensitization of Er^{3+} by fluorescein. The $^4F_{9/2}$ level of Er^{3+} (at 15 500 cm^{-1}) could be an additional pathway in the fluorescein complex. Moreover, the decrease in fluorescence of fluorescein is stronger than in the eosin and erythrosin fluorescence deactivation (Table 3), which is a second reason for the higher sensitization efficiency by fluorescein.

For Yb^{3+}, fluorescein is found to be a more efficient sensitizer as well. The difference in sensitization of fluorescein compared to the other dyes is somewhat smaller than in the Nd^{3+} and Er^{3+} complexes. The fluorescence of eosin and erythrosin is less quenched than the fluorescence of fluorescein in **1R$_4$**.Yb (Table 3). The receiving energy level of Yb^{3+} can only be the $^2F_{5/2}$ at 10 200 cm^{-1}, as this is the only excited state of this ion. A Dexter type mechanism to this level is allowed by the selection rules, because $|\Delta J| = 1$. The energy gap between the triplet states of the sensitizers and this receiving level is about 4000 cm^{-1}, a gap that is not too large for energy transfer but is too large for energy back transfer. A photon-induced electron transfer[26] could be a pathway in the sensitization process, because Yb^{3+} is easily reduced to Yb^{2+}. However, this is not likely here because there is no different quenching effect on the fluorescence of the dyes in the Yb^{3+} complexes compared to other complexes (see above under fluorescence quantum yields and Table 3). Furthermore, the calculated driving force for charge transfer, according to Rehm and Weller,[61] is very small: −0.18 eV for transfer from the singlet excited state of fluorescein.[62] An additional argument is that in the Eu^{3+} complex, which is reduced more easily than Yb^{3+},[63] phosphorescence is observed. This leads to the conclusion that in the current work the sensitization of Yb^{3+} occurs by a Dexter mechanism from the triplet excited state of the dyes.

Conclusions

NIR emitting lanthanide complexes were designed and synthesized that bring the sensitizer in close proximity to the ion and that shield the ion completely from the solvent. The sensitizers coupled to lanthanide complexes are fluorescein, eosin, and erythrosin, which enable visible light (green) sensitization of the NIR lanthanide emission. The fluorescence of the sensitizers was strongly reduced, because of the enhancement in intersystem crossing by the nearby paramagnetic lanthanide ions. The sensitization of the NIR emitting ions is solely determined by the energy transfer step, because of the enhanced intersystem crossing quantum yields. However, the overall luminescence is in all cases largely determined by the low intrinsic quantum yield of the lanthanide ions. Surprisingly, the efficiency of sensitization was found the highest for the fluorescein complexes **1H$_4$**.Ln. In the **1R$_4$**.Nd complexes, it was found that the main channel for energy transfer is the $^4F_{9/2}$ Nd^{3+} level. Fluorescein is a more efficient sensitizers than eosin or erythrosin, because of the larger gap between the triplet of fluorescein with this receiving Nd^{3+} level which leads to less energy back transfer. In the Yb^{3+} complexes, the more efficient excitation is most likely due to the less efficient enhancement of the intersystem crossing of eosin and erythrosin. The reason of the more efficient sensitization by fluorescein in the Er^{3+} complexes is that an additional level of Er^{3+} is probably capable of accepting energy from fluorescein but not from eosin or erythrosin. As long as these sensitizers, and especially fluorescein, are in close proximity (<6 Å) to the energy accepting ions, the energy transfer is determined by the energy levels involved.

Acknowledgment. This research is supported by the Technology Foundation STW, applied science division of NWO and the technology program of the Ministry of Economic Affairs. Akzo Nobel is gratefully acknowledged for technical support. Hans Hofstraat, Philips research and University of Amsterdam, is acknowledged for providing help in the lifetime measurements in the near-infrared.

Supporting Information Available: A detailed description of the synthesis and the mass spectrometry characterization (ESI-

TOF) data of the complexes (Table 1) are presented. This material is available free of charge via the Internet at http://pubs.acs.org.

References and Notes

(1) For a review, see: Parker, D.; Williams, J. A. G. *J. Chem. Soc., Dalton Trans*. **1996**, 3613.

(2) De Sa, G. F.; Malta, O. L.; de Mello Donega, C.; Simas, A. M.; Longo, R. L.; Santa-Cruz, P. A.; da Silva, E. F., Jr. *Coord. Chem. Rev.* **2000**, *196*, 165.

(3) Steemers, F. J.; Verboom, W.; Reinhoudt, D. N.; van der Tol, E. B.; Verhoeven, J. W. *J. Am. Chem. Soc.* **1995**, *117*, 9408.

(4) Hemmilä, I. K. *Applications of Fluorescence in Immunoassays*; Wiley and Sons: New York, 1991.

(5) Klink, S. I.; Grave, L.; Reinhoudt, D. N.; van Veggel, F. C. J. M.; Werts, M. H. V.; Geurts, F. A. J.; Hofstraat, J. W. *J. Phys. Chem. A* **2000**, *104*, 5457.

(6) Klink, S. I.; Hebbink, G. A.; Grave, L.; van Veggel, F. C. J. M.; Reinhoudt, D. N.; Slooff, L. H.; Polman, A.; Hofstraat, J. W. *J. Appl. Phys.* **1999**, *86*, 1181.

(7) Hasegawa, Y.; Ohkubo, T.; Sogabe, K.; Kawamura, Y.; Wada, Y.; Nakashima, N.; Yanagida, S. *Angew. Chem., Int. Ed.* **2000**, *39*, 357.

(8) Beeby, A.; Faulkner, S. *Chem. Phys. Lett.* **1997**, *266*, 116.

(9) Maupin, C. L.; Dickins, R. S.; Govenlock, L. G.; Mathieu, C. E.; Parker, D.; Williams, J. A. G.; Riehl, J. P. *J. Phys. Chem. A* **2000**, *104*, 6709.

(10) Voloshin, A. I.; Shavaleev, N. M.; Kazakov, V. P. *J. Lumin.* **2001**, *93*, 115.

(11) Slooff, L. H.; Polman, A.; Oude Wolbers, M. P.; van Veggel, F. C. J. M.; Reinhoudt, D. N.; Hofstraat, J. W. *J. Appl. Phys.* **1998**, *83*, 497.

(12) Werts, M. H. V.; Woudenberg, R. H.; Emmerink, P. G.; van Gassel, R.; Hofstraat, J. W.; Verhoeven, J. W. *Angew. Chem., Int. Ed.* **2000**, *39*, 4542.

(13) Miniscalco, W. J. *J. Lightwave Technol.* **1991**, *9*, 234.

(14) For an early paper, see: Meshkova, S. B.; Rusakova, N. V.; Bolshoi, D. V. *Acta Chim. Hung.* **1992**, *129*, 317.

(15) Gschneidner, K. A.; Eyring, L. R. *Handbook on the Physics and Chemistry of Rare Earths*; North-Holland Publishing Company: Amsterdam, 1979.

(16) Lowe, M. P.; Parker, D. *Inorg. Chim. Acta* **2001**, *317*, 163.

(17) Vögtle, F.; Gorka, M.; Vicinelli, V.; Ceroni, P.; Maestri, M.; Balzani, V. *Chem. Phys. Chem.* **2001**, 769.

(18) Hebbink; G. H.; Klink; S. I.; Grave, L.; Oude Alink, P. G. B.; van Veggel, F. C. J. M. *ChemPhysChem.* **2002**, *3*, 1014.

(19) Sabbatini, N.; Guardigli, M.; Lehn, J.-M. *Coord. Chem. Rev.* **1993**, *123*, 201.

(20) One of the referees argued that it should be efficiency of luminescence instead of quantum yield, because this value was not measured directly. However, as stated it is correct notwithstanding the fact that this value was indeed measured indirectly.

(21) Sato, S.; Wada, M. *Bull. Chem. Soc. Jpn.* **1970**, *43*, 1955.

(22) Latva, M.; Takalo, H.; Mukkala, V. M.; Matachescu, C.; Rodriguez-Ubis, J. C.; Kankare, J. *J. Lumin.* **1997**, *75*, 149.

(23) Werts, M. H. V.; Duin, M. A.; Hofstraat, J. W.; Verhoeven, J. W. *Chem. Commun.* **1999**, 799.

(24) Dadabhoy, A.; Faulkner, S.; Sammes, P. G. *J. Chem. Soc., Perkin Trans. 2* **2000**, 2359.

(25) Stein, G.; Würzberg, E. *J. Phys. Chem.* **1975**, *62*, 208.

(26) Horrocks, W. DeW.; Bolender, J. P.; Smith, W. D.; Supkowski, R. M. *J. Am. Chem. Soc.* **1997**, *119*, 5972.

(27) Korovin, Y.; Rusakova, N. *Rev. Inorg. Chem.* **2001**, *21*, 299.

(28) Oude Wolbers, M. P.; van Veggel, F. C. J. M.; Peters, F. G. A.; van Beelen, E. S. E.; Hofstraat, J. W.; Geurts, F. A. J.; Reinhoudt, D. N. *Chem. Eur. J.* **1998**, *4*, 772.

(29) Werts, M. H. V.; Hofstraat, J. W.; Geurts, F. A. J.; Verhoeven, J. W. *Chem. Phys. Lett.* **1997**, *276*, 196.

(30) Klink, S. I.; Oude Alink, P.; Grave, L.; Peters, F. G. A.; Hofstraat, J. W.; Geurts, F. A. J.; van Veggel, F. C. J. M. *J. Chem. Soc., Perkin Trans. 2* **2001**, 363.

(31) Wong, W. K.; Hou, A.; Guo, J.; He, H.; Zhang, L.; Wong, W. Y.; Li, K. F.; Cheah, K. W.; Xue, F.; Mak, T. C. W. *J. Chem. Soc., Dalton Trans.* **2001**, 3092.

(32) Beeby, A.; Dickins, R. S.; FitzGerald, S.; Govenlock, L. J.; Maupin, C. L.; Parker, D.; Riehl, J. P.; Siligardi, G.; Williams, J. A. G. *Chem. Commun.* **2000**, 1183.

(33) Klink, S. I.; Keizer, H.; van Veggel, F. C. J. M. *Angew. Chem., Int. Ed.* **2000**, *39*, 4319.

(34) Dexter, D. L. *J. Chem. Phys.* **1953**, *21*, 836.

(35) Murov, S. L.; Carmichael, I.; Hug, G. L. *Handbook of photochemistry*, 2nd ed.; Marcel Dekker: New York, 1993.

(36) van Houten, J.; Watts R. J. *J. Am. Chem. Soc.* **1976**, *98*, 4853.

(37) Werts, M. H. V.; Verhoeven, J. W.; Hofstraat, J. W. *J. Chem. Soc., Perkin Trans. 2* **2000**, 433.

(38) Hebbink, G. A.; Reinhoudt, D. N.; van Veggel, F. C. J. M. *Eur. J. Org. Chem.* **2001**, 4101.

(39) Klink, S. I.; Hebbink, G. A.; Oude Alink, P. G. B.; Grave, L.; van Veggel, F. C. J. M.; Werts, M. H. V. *J. Phys. Chem. A* **2002**, *106*, 3681. (b) Hebbink, G. A.; Klink, S. I.; Oude Alink, P. G. B.; van Veggel, F. C. J. M. *Inorg. Chim. Acta* **2001**, *317*, 114.

(40) For the procedure, see: van Veggel, F. C. J. M.; Oude Wolbers, M. P.; Reinhoudt, D. N. *J. Phys. Chem. A* **1998**, *102*, 3060. For the Lennard Jones parameters for the lanthanide ions, see: van Veggel, F. C. J. M.; Reinhoudt, D. N. *Chem. Eur. J.* **1999**, *5*, 90.

(41) Jorgensen, W. L. *J. Phys. Chem.* **1986**, *90*, 1276 (OPLS stands for optimized potentials for liquid simulations).

(42) The central carbon atom of the xanthene unit, at the para position to the oxygen in the central ring, was taken as a measure of the distance.

(43) Slooff, L. H.; Polman, A.; Klink, S. I.; Hebbink, G. A.; Grave, L.; van Veggel, F. C. J. M.; Reinhoudt, D. N.; Hofstraat, J. W. *Opt. Mater.* **2000**, *14*, 101. Slooff, L. H.; Polman, A.; Hebbink, G. A.; van Veggel, F. C. J. M.; Reinhoudt, D. N.; Cacialli, F.; Friend, R. H. *Appl. Phys. Lett.* **2001**, *78*, 2122.

(44) Horrocks, W. DeW.; Sudnick, D. R. *Acc. Chem. Res.* **1981**, *14*, 384.

(45) Beeby, A.; Clarkson, I. M.; Dickins, R. S.; Faulkner, S.; Parker, D.; Royle, L.; de Sousa, A. S.; Williams, J. A. G.; Woods, M. *J. Chem. Soc., Perkin Trans. 2* **1999**, 493.

(46) Klink, S. I.; Hebbink, G. A.; Grave, L.; Peters, F. G. A.; van Veggel, F. C. J. M.; Reinhoudt, D. N.; Hofstraat, J. W. *Eur. J. Org. Chem.* **2000**, 192.

(47) The low-energy side of the $^4F_{3/2} \rightarrow {}^4I_{13/2}$ transition of Nd^{3+} at 1330 nm is distorted by absorption around 1400 nm, which is the first overtone of the 2950 cm^{-1} C−H vibration of the solvent (CH_3OD).

(48) Ermolaev, V. L.; Sveshnikova, E. B. *Russ. Chem. Rev.* **1994**, *63*, 905.

(49) Weber, M. J. *Phys. Rev.* **1968**, *168*, 283.

(50) Polman, A. *Physica B* **2001**, *300*, 78.

(51) The energy levels of the three dyes, the 0−0 transitions of the singlet and the triplet states, were determined from the spectra and are represented in Figure 1. The 0−0 transitions of the singlet state are estimated as the crossing of the absorption and fluorescence spectra. The 0−0 of the triplet state was estimated from crossing of the singlet−triplet excitation spectrum and the phosphorescence spectrum of **1R4**.Gd at 77 K. Although the singlet−triplet absorption is relative weak, the excitation spectrum could easily be distinguished from the singlet−singlet excitation of the phosphorescence (cf. ref 35 p 54).

(52) Delayed detection was accomplished by equipping the spectrofluorimeter with a rotating drum. Doing so, a delay between excitation and emission of about 2 ms was accomplished. Compare ref 37.

(53) Tobita, S.; Arakawa, M.; Tanaka, I. *J. Phys. Chem.* **1984**, *88*, 2697. Tobita, S.; Arakawa, M.; Tanaka, I. *J. Phys. Chem.* **1985**, *89*, 5649.

(54) Guldi, D. M.; Mody, T. D.; Gerasimchuk, N. N.; Magda, D.; Sessler, J. L. *J. Am. Chem. Soc.* **2000**, *122*, 8289.

(55) Gonçalves e Silva, F. R.; Malta, O. L.; Reinhard, C.; Güdel, H. U.; Piguet, C.; Moser, J. E.; Bünzli, J.-C. G. *J. Phys. Chem. A* **2002**, *106*, 1670.

(56) Blasse, G.; Grabmaier B. C. *Luminescent materials*; Springer-Verlag: Berlin, 1994.

(57) The $^7H_{11/2}$ level of Nd^{3+} can be an acceptor level because of the selection rules. However, this level is higher in energy than the triplet states of the sensitizers and is therefore not taken in to account.

(58) Sato, S.; Wada, M. *Bull. Chem. Soc. Jpn.* **1970**, *43*, 1955.

(59) The assumption here is that all other energy conversion processes are not temperature-dependent. This is not completely true, but the effects are much smaller than the temperature dependence of the back-tranfer rate (Turro, N. J. *Modern Molecular Photochemistry*; The Benjamin/Cummings Publishing Co., Inc.: Menlo Park, CA, 1978).

(60) Payne, S. A.; Bibeau, C. *J. Lumin.* **1998**, *79*, 143.

(61) Rehm, D.; Weller, A. *Isr. J. Chem.* **1970**, *8*, 259.

(62) $-\Delta G = -E(\text{dye}^{\bullet+}/\text{dye}) + E_{\text{dye}^*} + E(Yb^{3+}/Yb^{2+})$; $E(\text{dye}^{\bullet+}/\text{dye}) =$ 1.14 V vs NHE (Jones, G., III.; Qian, X. *J. Photochem. Photobiol. A: Chem.* **1998**, *113*, 125), $E(Yb^{2+}/Yb^{3+}) = 1.05$ V vs NHE (Lide, D. R., Ed.; *Handbook of Chemistry and Physics*, 76th ed.; CRC Press: Boca Raton, FL, 1996). The oxidation potential of Yb^{3+} is expected to be even higher as the triple charged ion is stabilized by the ligand. This leads to even lower values of the driving force.

(63) $E(Eu^{3+}/Eu^{2+}) = -0.35$ V (vs NHE), $E(Yb^{3+}/Yb^{2+}) = -1.05$ V (vs NHE), Lide, D. R., Ed.; *Handbook of Chemistry and Physics*, 76th ed.; CRC Press: Boca Raton, FL, 1996.